Presurgical thalamocortical connectivity is associated with response to vagus nerve stimulation in children with intractable epilepsy

George M. Ibrahim[c,*], Priya Sharma[d], Ann Hyslop[d], Magno R. Guillen[e], Benjamin R. Morgan[f], Simeon Wong[g], Taylor J. Abel[a], Lior Elkaim[h], Iahn Cajigas[a,b], Ashish H. Shah[a,b], Aria Fallah[h], Alexander G. Weil[i], Nolan Altman[e], Byron Bernal[e], Santiago Medina[e], Elysa Widjaja[g], Prasanna Jayakar[d], John Ragheb[a,b], Sanjiv Bhatia[a,b]

[a] Division of Neurosurgery, Brain Institute, Nicklaus Children's Hospital, Miami, FL, USA
[b] Division of Neurosurgery, University of Miami/Miller School of Medicine, Miami, FL, USA
[c] Division of Neurosurgery, Department of Surgery, Hospital for Sick Children, University of Toronto, Toronto, ON, Canada
[d] Department of Neurology, Brain Institute, Nicklaus Children's Hospital, Miami, FL, USA
[e] Department of Radiology, Nicklaus Children's Hospital, Miami, FL, USA
[f] Faculty of Medicine, University of Toronto, Toronto, ON, Canada
[g] Division of Diagnostic Imaging, Hospital for Sick Children, Toronto, ON, Canada
[h] Department of Neurosurgery, Mattel Children's Hospital, David Geffen School of Medicine at University of California Los Angeles, Los Angeles, California, USA
[i] Division of Neurosurgery, CHU Sainte-Justine Hospital, University of Montreal, Montreal, QC, Canada

ARTICLE INFO

ABSTRACT

Although chronic vagus nerve stimulation (VNS) is an established treatment for medically-intractable childhood epilepsy, there is considerable heterogeneity in seizure response and little data are available to pre-operatively identify patients who may benefit from treatment. Since the therapeutic effect of VNS may be mediated by afferent projections to the thalamus, we tested the hypothesis that intrinsic thalamocortical connectivity is associated with seizure response following chronic VNS in children with epilepsy. Twenty-one children (ages 5–21 years) with medically-intractable epilepsy underwent resting-state fMRI prior to implantation of VNS. Ten received sedation, while 11 did not. Whole brain connectivity to thalamic regions of interest was performed. Multivariate generalized linear models were used to correlate resting-state data with seizure outcomes, while adjusting for age and sedation status. A supervised support vector machine (SVM) algorithm was used to classify response to chronic VNS on the basis of intrinsic connectivity. Of the 21 subjects, 11 (52%) had 50% or greater improvement in seizure control after VNS. Enhanced connectivity of the thalami to the anterior cingulate cortex (ACC) and left insula was associated with greater VNS efficacy. Within our test cohort, SVM correctly classified response to chronic VNS with 86% accuracy. In an external cohort of 8 children, the predictive model correctly classified the seizure response with 88% accuracy. We find that enhanced intrinsic connectivity within thalamocortical circuitry is associated with seizure response following VNS. These results encourage the study of intrinsic connectivity to inform neural network-based, personalized treatment decisions for children with intractable epilepsy.

1. Introduction

Despite the widespread application of vagus nerve stimulation (VNS) to the treatment of medically-intractable epilepsy, results from implantation are heterogeneous and there are no established pre-operative guidelines to identify patients who may benefit from therapy. Although the mechanism of action of chronic VNS is poorly understood,

the thalamus has been previously implicated in its therapeutic effect (Narayanan et al., 2002; Liu et al., 2003). Direct projections from the vagus nerve to the thalami have been reported (Beckstead et al., 1980) and early electrophysiological studies in animals demonstrated widespread electrocorticographic changes consistent with thalamic modulation with VNS (Chase et al., 1966). In humans, VNS stimulation has been associated with increases in blood flow in the thalamus and

cingulate cortex (Ko et al., 1996; Henry et al., 1999; Henry et al., 2004). Data from event-related functional MRI studies also support a role for activation of the thalamus, basal ganglia and insular cortices with active stimulation (Narayanan et al., 2002), which may be linked to seizure response (Liu et al., 2003).

The individual patient response to stimulation is highly variable and unpredictable. A meta-analysis of randomized controlled trials of VNS encompassing 439 adults and children demonstrated heterogeneity in outcomes with > 50% seizure reduction in fewer than half of implanted patients (Panebianco et al., 2015). Furthermore, in pediatric populations, these rates may be as low as a 25% (Klinkenberg et al., 2012), implying that the majority of treated children accept surgical risk with a low likelihood of benefit. Intrinsic neuronal connectivity represents an attractive theoretical substrate to explain such clinical heterogeneity (Zhang and Raichle, 2010) and has been empirically used to classify neurocognitive disorders by their treatment response (Drysdale et al., 2017).

Given the confluence of data suggesting: (i) a mediatory role for thalamic networks in the therapeutic effect of VNS; (ii) a greater awareness of individual variability in therapeutic responses subserved by unique intrinsic connectivity; and (iii) the heterogeneous outcomes reported after VNS, we performed the first study to examine the relationship between large-scale network functional connectivity and seizure response to VNS. We hypothesize that intrinsic thalamocortical connectivity may be associated with seizure outcomes following stimulation, which may be used to identify patients who are most likely to benefit from VNS therapy.

In order to investigate these relations, resting-state fMRI data were obtained from children prior to implantation of VNS and patterns of intrinsic connectivity were associated with post-operative response to stimulation. Ten of the 21 children underwent imaging under propofol anesthesia, which is increasingly commonplace for clinical pediatric populations. It has been established that sedation attenuates low-frequency fluctuations of BOLD signal, preferentially in the anterior frontal and mesial temporal regions (Huang et al., 2014; Barttfeld et al., 2015). Specific to the thalamus, decreases in centrality (or hub-like network properties) have been noted with propofol anesthesia (Gili et al., 2013). In order to minimize the effects of sedation on our findings, we ensured that (i) sedated and non-sedated children were distributed between responders and non-responders to VNS, (ii) the binarized sedation status was included in all multivariable models, and (iii) subgroup analyses were performed for each cohort independently.

2. Methods

2.1. Patient population

Twenty-one children with medically-intractable epilepsy were recruited from the Miami (Nicklaus) Children's Hospital, a tertiary and quaternary care centre for the treatment of childhood epilepsy. Inclusion criteria for the study were children 21 years or younger who underwent VNS insertion and a resting-state fMRI study prior to the procedure. The participants ranged in age from 5 to 21 years. The seizure etiology was mostly unknown, although several presented with encephalitis. Seizure semiologies were often multiple and ranged from focal motor and non-motor seizures to generalized types. The majority of the ictal and interictal electroencephalograms revealed multifocal or generalized seizures and interictal discharges, respectively (see Supplementary Material for details). Only one subject had undergone a previous resective treatment, a neocortical anterior temporal lobectomy, which did not affect registration of functional and anatomical datasets or sampling of thalamic regions of interest. In addition, his fMRI study did not demonstrate any significant change in the canonical neural spontaneous networks.

Data for a separate group of eight children were collected in order to test the predictive model in an external cohort. Five of these children underwent resting-state fMRI studies at the Hospital for Sick Children (Toronto, Canada), while an additional three were recruited from the Miami (Nicklaus) Children's hospital. The inclusion criteria for the external cohort was less stringent than the test cohort. All children were under 21 years of age and included those who had undergone a prior frontal resection ($n = 1$), cortico-amygdalohippocampectomy (n = 1), and post-central resection (n = 1). One patients underwent a sedated resting-state study. Imaging for this multi-institutional cohort was acquired with varying parameters. The imaging parameters for this cohort are presented in the Supplementary Materials.

The current study was approved following Research Ethical Board review. For all prospectively collected fMRI studies, consent was obtained from subjects 18 years or older, or by the legally authorized representative for subjects under the age of 18. Assent was also required of subjects between the ages of 13 and 17. A separate Research Ethical Board approval was sought and obtained in order to also include studies meeting the inclusion criteria that had been retrospectively collected. The study complies with the Code of Ethics of the World Medical Association (Declaration of Helsinki).

2.2. Clinical covariates

All children within the test cohort were implanted with VNS supplied by Cyberonics Inc. In all cases, the stimulation was titrated according to the seizure diaries maintained by patients to optimal efficacy. The primary outcome of interest was seizure response at last follow-up, which was defined as the percentage change in seizure frequency from baseline following VNS. In concordance with previous literature, children with 50% or greater decrease in seizure frequency were defined as good responders to therapy, while those with < 50% decrease were defined as poor responders (Panebianco et al., 2015; Klinkenberg et al., 2012). Seizure response was measured at least one year following VNS implantation, with the exception of two patients who had already achieved good seizure response within 6 months of implantation.

Ten children of the 21 were sedated for the fMRI study. These children received propofol anesthesia at a rate of 100 mcg/kg/min. Sedation status was considered a binary variable and included in all generalized linear models (below). Furthermore, subgroup analyses were performed for sedated and non-sedated patient cohorts separately (see Supplementary Materials).

2.3. Functional MRI acquisition and preprocessing

For the test cohort, structural and functional MRI data were collected from 2009 to 2015 on patients who subsequently underwent VNS insertion. Data were collected using a 1.5T scanner (Intera magnet; Philips Healthcare, Best, the Netherlands) with a single channel transmit/receive head coil. Patients were imaged using volumetric 3D T1 (TR/TE = 4.9/2.3 ms, section thickness = 1 mm, FOV = 22 cm, matrix = 256 × 256), and resting state fMRI (EPI, TR/TE = 2000/60 ms, matrix = 64 × 64 voxel, voxel size = 3.75 × 3.75 × 4.5 mm, 150 time points acquired). Non-sedated subjects were instructed to keep their eyes closed and not to focus on anything in particular during the study.

The functional data were analyzed using standard FMRIB Software Library (FSL) tools (Jenkinson et al., 2002). Slice-timing and motion correction were performed and the functional data was aligned to each subject's high-resolution anatomical T1-weighted images. Data underwent spatial smoothing using a 5 mm FWHM Gaussian kernel and was bandpass filtered with a lower cut-off frequency of 0.01 Hz. A general linear model was employed to regress the time course of cerebrospinal fluid, white matter, global signal and six-parameter motion maximum displacement time courses. Visual inspection of ICA maps was also used to denoise the data (Kelly et al., 2010). Single subject ICA was performed and structured noise was identified visually using (i) spatial

maps, by excluding components which appeared non-biological (at brain edges, or in white matter or CSF); (ii) time course, by excluding components with large spikes, saw-tooth patterns or drifts; and (iii) the power spectrum, where components were excluded if 50% of the power in the frequency spectrum was above 0.1 Hz.

2.4. Hypothesis-driven seed-based analysis

In order to test the hypothesis that unique patterns of thalamocortical connectivity are associated with seizure response following VNS, thalamic regions of interest (left and right) were defined by manually creating ROIs using the high-resolution T1 anatomical images of the different subjects. Two authors (L.E. and G.M.I.) manually drew and verified thalamic ROIs. This manual step was performed in order to account for variability in anatomy, particularly in younger children. First-level analysis was performed by correlating the mean time series of the ROIs with the time series of all voxels in the brain. This analysis was performed using FEAT Version 5.98, part of FSL (www.fmrib.ox.ac.uk/fsl). Timeseries statistical analysis was carried out using FILM with local autocorrelation correction (Woolrich et al., 2001).

Mixed-effects higher-level analysis was subsequently performed to contrast the first level statistical parameter connectivity maps between good and poor responders to therapy, while controlling for several variables in the generalized linear model: the child's sedation state, age and sedation * response interaction. Spatial normalization to the MNI atlas was performed for higher-level analysis. This whole-brain analysis was performed using default parameters of FLAME 1 higher level analysis in FSL. These algorithms rely on Gaussian random field theory for family-wise error rate (FWE) corrected voxel-wise and cluster-wise inference. Statistical images were thresholded using clusters determined by $Z > 2.3$ and a (corrected) cluster significance threshold of $P < 0.05$ (Worsley, 2001).

2.5. Support vector machine classification of seizure response on the basis of intrinsic connectivity

A supervised support vector machine (SVM) learning algorithm was utilized by supplying a known set of inputs and known responses to the data (seizure response to VNS dichotomized as good and poor) (Christianini and Shawe-Taylor, 2000). In order to compute the inputs for the SVM, the clusters demonstrating significant connectivity to both the left and right thalamus were overlaid. The significant clusters were trimmed to compute masks for regions demonstrating significant connectivity to both thalami, the ACC/vmPFC and the left insula. Masks were then transformed to each individual subject's functional space and the time series of the masks were extracted for each patient. The inputs for the classifier consisted of four correlation coefficients between the timeseries of the thalami to the significant clusters (ACC/vmPFC and left insula). Only clusters demonstrating significant connectivity to both thalami were considered in the SVM in order (i) to decrease the number of inputs to the model; and (ii) to decrease the possibility of a Type I error by considering clusters significantly connected to both thalami as being brain regions expressing thalamocortical interactions that are robustly associated with treatment response.

The data were used to train a model that generates predictions for the response to new data. A linear SVM classifier was utilized by finding the best hyperplane that separates all data points of one class from those of the other class. The best hyperplane is characterized by the largest margin between the two classes, whereby margin indicates the maximal width of the slab parallel to the hyperplane with no interior data points (Christianini and Shawe-Taylor, 2000).

In order to cross-validate the model, the data were partitioned into 5 folds (or division), which were held out in turn for testing. Using fewer fold partitions did not affect the accuracy of the classifier. A model was trained for each fold using all the data outside the fold. The function then tested each model performance using the data inside the fold and

Table 1
Summary of patient demographics, stratified by response to VNS.

Variable	≥ 50% seizure improvement (percent) ($n = 11$)	< 50% seizure improvement (percent) ($n = 10$)	p-value*
Age (years)			
0–5	1 (10)	1 (10)	0.99
6–10	2 (18)	2 (20)	
11–21	8 (72)	7 (70)	
Seizure semiology			
Focal motor	6 (55)	5 (50)	0.92
Focal non-motor	6 (55)	5 (50)	
Generalized motor	4 (36)	4 (40)	
Generalized absence	1 (9)	2 (20)	
Seizure frequency (pre-VNS)			
Daily	6 (55)	6 (60)	0.62
Weekly	4 (36)	4 (40)	
Monthly	1 (9)	0	
Total number of attempted AEDs			
	8 ± 3	6 ± 2	0.13
Etiology			
Encephalitis	5 (45)	1 (10)	0.27
IGE**	0	1 (10)	
Genetic	1 (9)	1 (10)	
Unknown	5 (45)	7 (70)	
Imaging findings			
Normal***	3 (27)	5 (50)	0.28
Encephalomalacia	8 (73)	5 (50)	
Sedation at fMRI			
Sedated	4 (36)	6 (60)	0.28
Non-sedated	7 (64)	4 (40)	
Time to last follow-up			
6–11 months	2 (18)	0	0.48
> 1 year	9 (64)	10 (70)	

* Based on Chi-squared test.
** Denotes idiopathic generalized epilepsy.
*** Excludes incidental findings, such as Chiari malformations and developmental venous anomalies.

calculated the average test error over all the folds. A receiver-operator characteristics curve was then plotted to demonstrate the sensitivity and specificity of the SVM model in identifying patients within the tested cohort who benefited from VNS on the basis of intrinsic connectivity. The classifier was then tested on a multi-institutional cohort of eight additional patients. Description of this cohort can be found in the Supplementary Materials. All analyses were performed in MATLAB version 2015a (The Mathworks, Natrick MA) using built-in functions and custom in-house scripts as well as R statistical software.

3. Results

Of the 21 children within the test cohort, 11 (52%) achieved a good seizure response to chronic VNS (> 50% seizure reduction from baseline). The subject demographics, including seizure characteristics and neuroimaging findings are summarized in Table 1 (also refer to Supplementary Fig. 1 and Supplementary Tables S1, S2 and S3). Pre- and post-VNS seizure frequency is reported for each patient in Supplementary Table S2. Both qualitatively and statistically, there was no difference in the pre-operative seizure frequency among responders and non-responders to VNS. Only two patients achieved seizure-freedom following VNS. There were no significant differences between responders and non-responders to VNS with respect to any clinical, electrophysiological or imaging covariates.
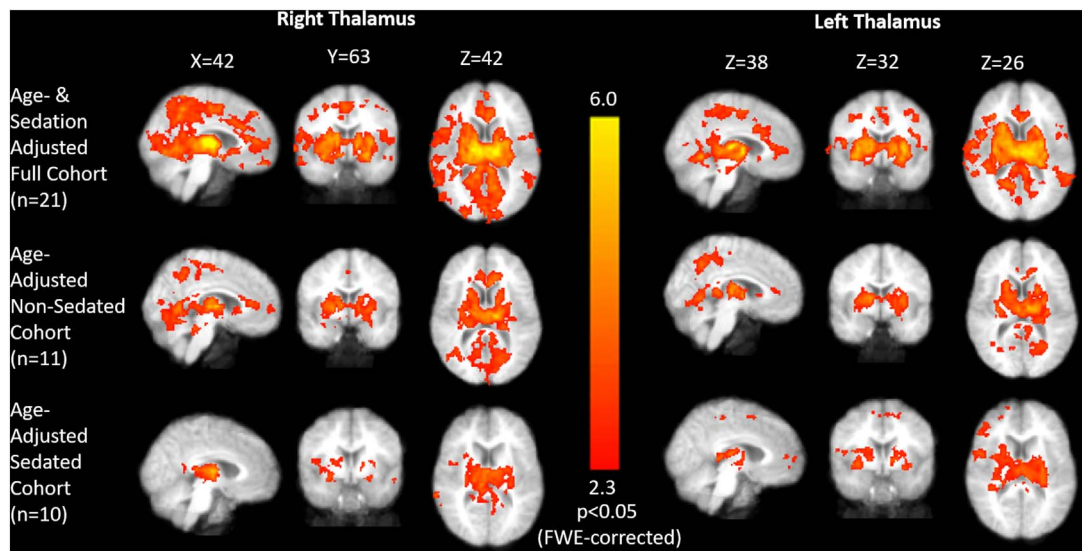
Fig. 1. Whole-brain connectivity to right and left thalamic regions of interest. Seed-based analysis demonstrates widespread connectivity of the thalamus to cortical and subcortical regions in the entire cohort and the subset of patients who were and were not sedated. Mean statistical Z-maps (FWE-corrected) are shown with all analyses adjusted for patient age and main results (top panel) also adjusted for binarized sedation status.

3.1. Children with good response to VNS demonstrate greater thalamocortical connectivity involving the cingulate and insular cortex

Whole-brain connectivity analysis was performed by correlating the timeseries of thalamic regions of interest with the time series of all brain voxels in functional space. The mean statistical parametric maps of thalamic to whole brain connectivity reveal diffuse connectivity of the thalamus to cortical and subcortical structures (Fig. 1). When the timeseries of the left thalamus was correlated with all brain voxels, two significant clusters were identified, representing stronger thalamocortical connectivity in patients with good response to VNS, compared to those with poor response. Significant differences were expressed in the connectivity between the left thalamus and the anterior cingulate/ ventromedial prefrontal cortex (ACC/vmPFC) and bilateral operculo-insular cortex (Fig. 2; $p < 0.05$, corrected). These effects were dissociable within the multivariate generalized linear model from age-related effects, sedation effects and bivariate interactions. With increasing age, greater connectivity of the left thalamus to the precuneus, ACC/ vmPFC, and right operculo-insular, parieto-occipital and peri-Rolandic cortices. There was no significant pattern of thalamocortical connectivity related to sedation effect or any significant interactions within the generalized linear model.

When a second region of interest was placed within the right thalamus and correlated with the timeseries of all brain voxels, children with good seizure response to VNS were found to exhibit greater connectivity of the ROI to the ACC/vmPFC and left insular cortex than those with poor response (Fig. 3; $p < 0.05$, corrected). Once again, this effect was dissociable from an age-effect, whereby greater connectivity of the right thalamus to the left operculo-insular cortex was observed. No significant sedation effects or interactions were identified. Although no main effects or interactions for sedation were identified, subgroup analyses were performed within the cohort of children who were and were not sedated to ensure that our findings were robust. In each of these subgroup analyses, regions of the cingulate and/or left insular cortices were consistently associated with seizure response to VNS (Supplementary Figs. S2 and S3 and Supplementary Tables S5 and S6).

3.2. The seizure response of children with epilepsy may be accurately classified on the basis of intrinsic connectivity

A linear SVM classifier was trained using the correlation coefficients

of the relationship between the thalami and anterior cingulate and left insular cortex. The distribution of correlation values for these relations in responders and non-responders to VNS is presented in Fig. 4. A stronger positive correlation between the thalami and these regions was consistently demonstrated in the responders to VNS, relative to the non-responders.

The masks representing the significant clusters for the two brain regions expressing differential thalamocortical connectivity in responders and non-responders to VNS are presented in Supplementary Fig. S4. Correlations among these masked regions and the thalami were used as inputs for the SVM. The data were used to train a model for prediction of outcome using a 5 fold partition for cross-validation. The classification model yielded 86% accuracy in classifying patients in our test cohort as good versus poor responders on the basis of thalamocortical connectivity (Fig. 5). A Receiver-Operator Characteristics curve for the identification of good responders is presented in Fig. 5C (AUC 0.86).

3.3. Prediction of seizure response in an external cohort of children undergoing VNS

The SVM predictive model was applied to a multi-institutional cohort of 8 children who underwent VNS (ages 5–18). The demographic information for these children is presented in Supplementary Tables S8 and S9. All subjects except for one underwent the imaging study without sedation. Within the external cohort, 7 achieved good seizure response to VNS, while a single participant did not. When the trained model was applied to the external cohort, the seizure response of 7 of the 8 children was correctly classified (Fig. 5A and Fig. 5B; 88% accuracy).

4. Discussion

Although vagus nerve stimulation is increasingly commonplace in the treatment of intractable childhood epilepsy, its mechanism of action is poorly understood and it remains unclear why some children respond better to chronic VNS than others. Here, we explore the correlation of intrinsic thalamocortical connectivity using pre-operative resting-state fMRI with seizure response following chronic VNS. Our study suggests several novel findings: (i) thalamocortical connectivity to the anterior cingulate and insular cortices is significantly stronger in patients who
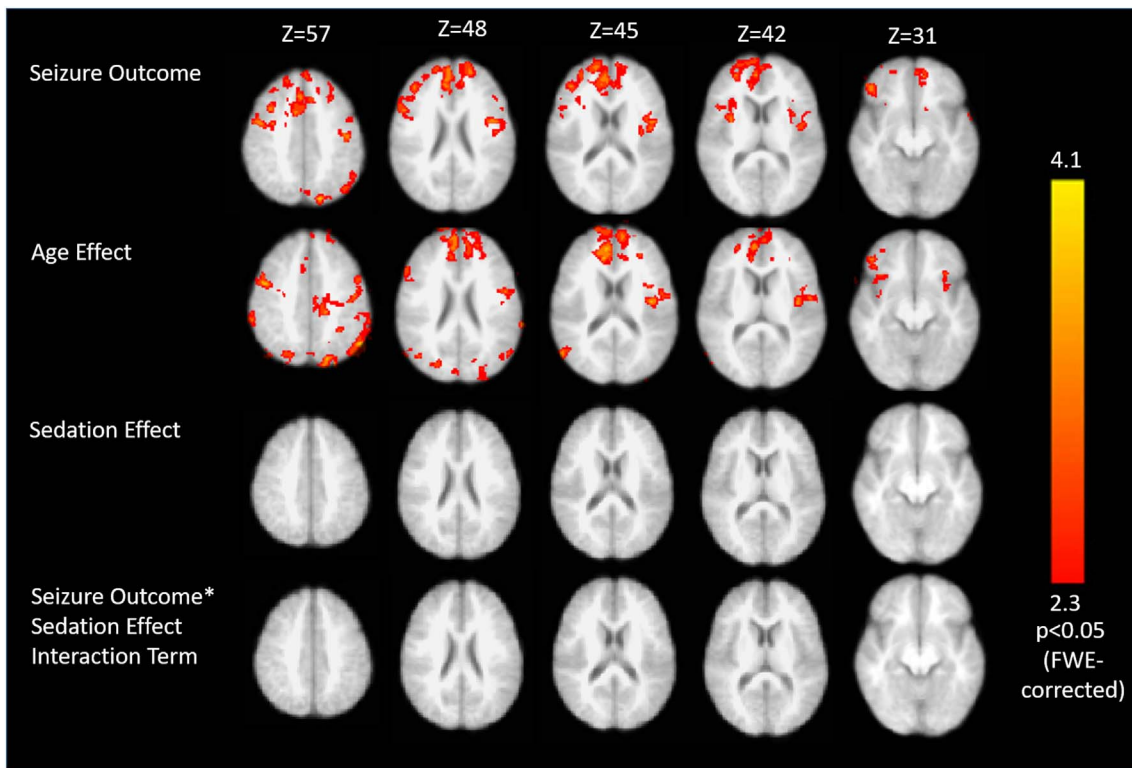
Fig. 2. Generalized linear model of left thalamic whole-brain connectivity regressed against selected covariates. In children with good seizure response to VNS, the left thalamus is significantly more strongly connected to the anterior cingulate and bilateral operculo-insular cortices as well as the parietooccipital junction and peri-Rolandic cortex (top panel). This effect was dissociable from age-related differences in connectivity to the left thalamus (second panel). There was no significant sedation effect or interaction (lower panels). All clusters shown are significant at $p < 0.05$ following FWE-correction for multiple comparisons.
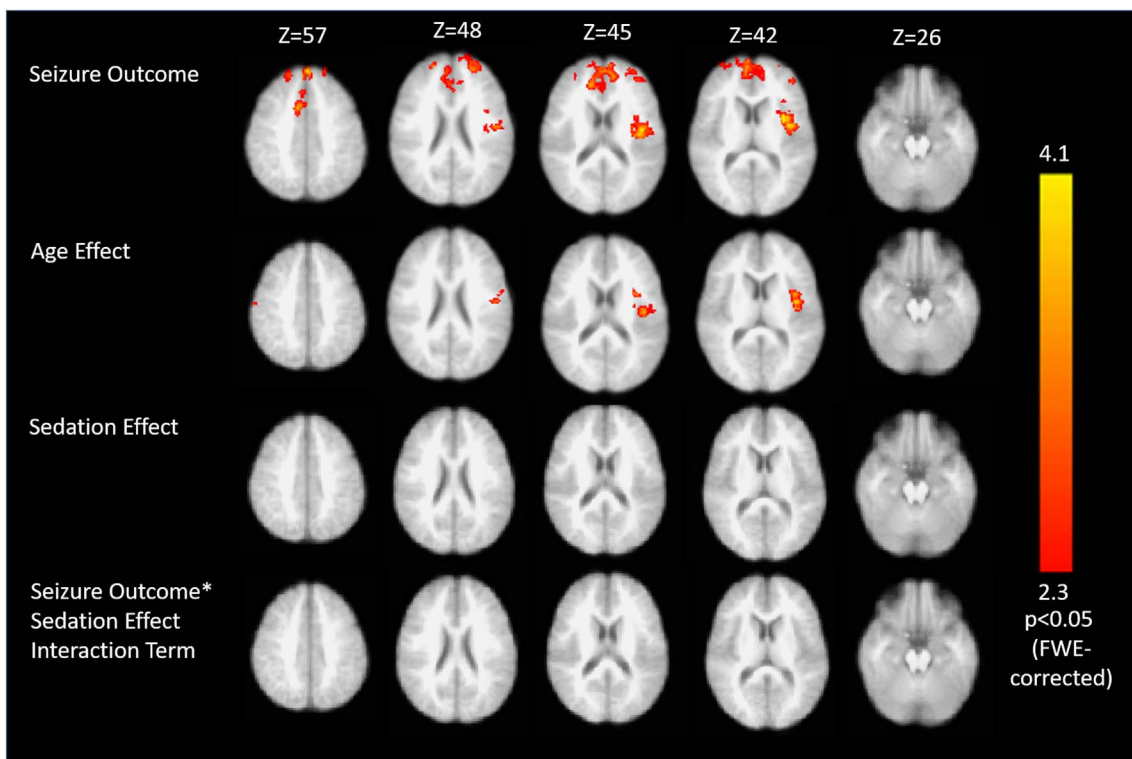

Fig. 3. Generalized linear model of right thalamic whole-brain connectivity regressed against selected covariates. In children with good seizure response to VNS, the right thalamus is significantly more strongly connected to the anterior cingulate and left insular cortices (top panel). Again this effect was dissociable from age-related differences in connectivity to the right thalamus (second panel). There was no significant sedation effect or interaction (lower panels). All clusters shown are significant at $p < 0.05$ following FWE-correction for multiple comparisons.
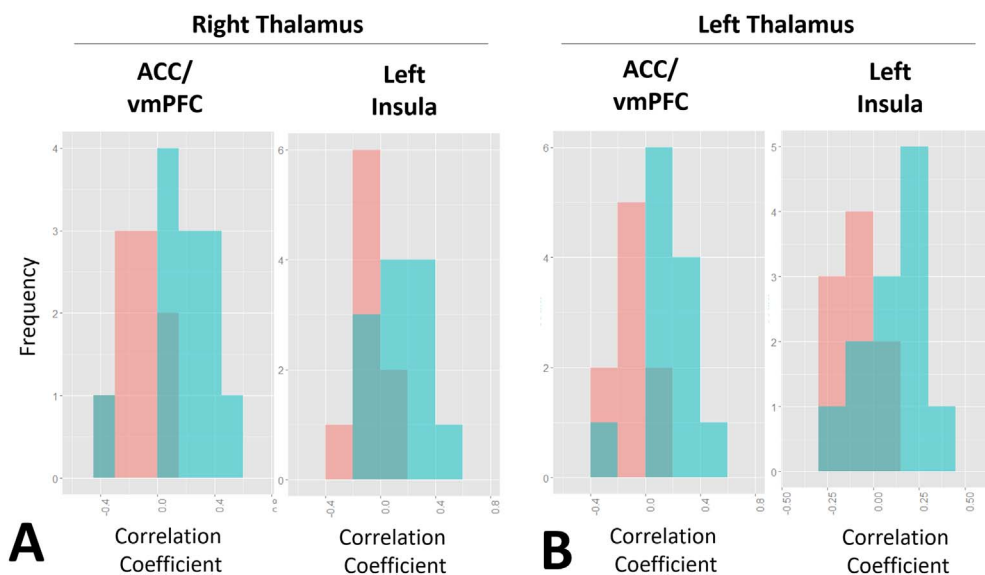
Fig. 4. Distribution of thalamo-cinguate and thalamo-insular connectivity correlation coefficients in responders and non-responders to VNS. For all brain regions expressing significant thalamocortical connectivity, the responders to VNS demonstrated higher positive correlation than non-responders. Blue denotes good, while pink denotes poor response to VNS.

demonstrate a good response to VNS; (ii) response to VNS may be accurately predicted using support vector machine classifiers on the basis of intrinsic functional connectivity; (iii) the findings of the classifier may be generalized, at least in a small cohort of subjects, from an independent institution. The current findings have important implications for the treatment of intractable epilepsy in children via neuromodulatory strategy and strongly suggest a role for connectomics in the delivery of patient-specific treatment strategies.

4.1. Thalamocortical circuitry and the efficacy of vagus nerve stimulation

The vagus nerve carries general somatic afferent (GSA), general visceral afferent (GVA) and efferent fibres. The majority of the fibres of the vagus nerve are comprised of GVA (Rutecki, 1990). The afferent fibres project primarily to the nucleus of the solitary tract (NST) with other connections to the medial reticular formation (Rutecki, 1990). Ascending visceral information is relayed through the parabrachial

nucleus to the contralateral thalamus, and with left vagus nerve stimulation, cellular firing in the contralateral thalamus has been directly recorded (Saleh and Cechetto, 1993). Furthermore, studies with autoradiographic anterograde fiber-tracing with horseradish peroxidase retrograde cell labeling of the NTS demonstrated projections to the contralateral thalamus via the central tegmental tract (Beckstead et al., 1980).

The finding that thalamocortical connectivity is enhanced in children demonstrating good response to VNS is consistent with literature implicating thalamocortical circuitry in the therapeutic effect of stimulation (Fisher et al., 2010). Henry and colleagues reported an anecdotal association between seizure outcomes and VNS-induced decreases in cortical CBF and increases in thalamic CBF (Henry et al., 2004). VNS-induced activation of the thalamus has also been associated with seizure response in event-related fMRI studies (Liu et al., 2003). Furthermore, Naritoku and colleagues report interval increases in the latency of thalamocortical somatosensory evoked potentials in
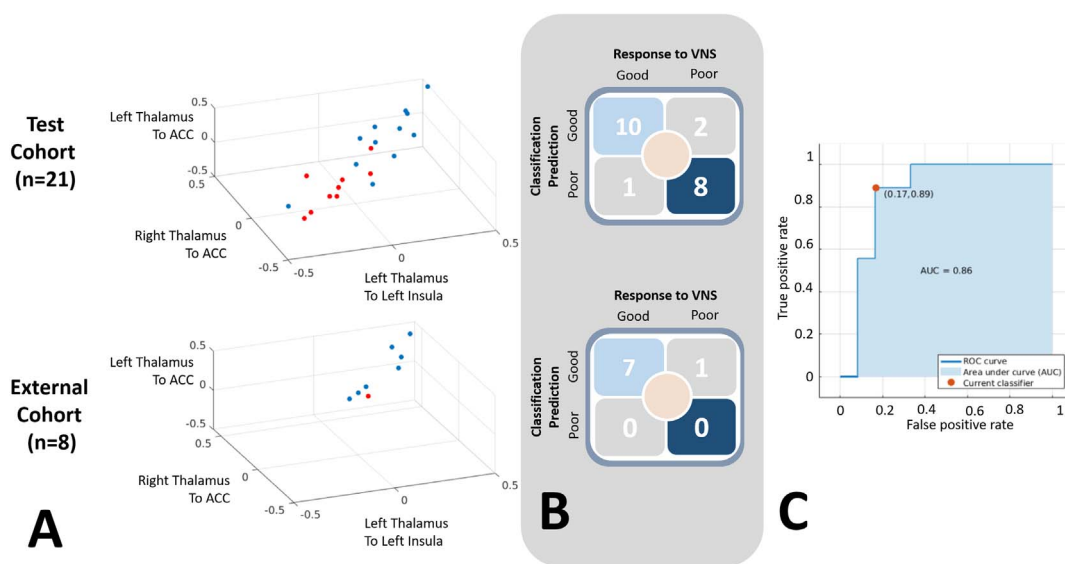

Fig. 5. Support vector machines accurately classify response to VNS on the basis of intrinsic thalamocortical connectivity. (A) Classification of response to VNS on the basis of thalamocortical connectivity for the test and external cohorts. Blue denotes good, while red denotes poor response to VNS. Three of the four thalamocortical pair-wise connectivity correlation coefficients used as inputs in the SVM are shown. (B) On the basis of thalamocortical connectivity to the anterior cingulate and left insular cortices, linear support vector machines classified seizure response to VNS with an 86% accuracy in the test cohort ($n = 21$) and 88% in the external cohort ($n = 8$). (C) The ROC curve for the ability to identify VNS responders within the test cohort s shown in top right panel (AUC: 0.86).

subcohorts of patients treated with chronic VNS (Naritoku et al., 1992). Interestingly, these velocities were slower in patients with epilepsy, compared to healthy controls, implying a baseline difference in thalamocortical circuitry. The convergent and reproducible finding that thalamic activation, which itself is inconsistently identified in subjects treated with VNS, is linked to seizure response supports the investigation of thalamocortical connectivity as a putative explanation for the heterogeneity in outcomes following VNS.

Consistent with our findings, previous authors have implicated the cingulate and insular cortices in the therapeutic effects of VNS, although the relations between presurgical connectivity and therapeutic response have not yet been examined. A study of VNS-induced *fos* expression demonstrated increased *fos* in the cingulate gyrus and amygdala (Naritoku et al., 1995). Furthermore of many cortical regions activated during a VNS-induced event-related fMRI, Narayanan found that activation of the insular cortices was the most robust. The same study identified consist thalamic activation bilaterally (left greater than right). Our findings of connectivity in low-frequency BOLD oscillations within these brain regions relate to seizure response complement previous activation studies.

4.2. The thalamus in childhood epilepsy

The observation that thalamocortical interactions are related to response to neuromodulation are also in concordance with previous studies showing increases in the strength of intrinsic connectivity within thalamocortical circuitry in children who achieve seizure freedom following epilepsy surgery (Ibrahim et al., 2015). We have previously shown that seizure freedom following disconnection procedures in children with epilepsy is associated with enhancement of thalamocortical connectivity (Ibrahim et al., 2015) and that the thalamus is a weaker hub in children with more severe epilepsy syndromes (Ibrahim et al., 2014a). Epileptiform dynamics originating in cortical regions are also known to initiate oscillations within thalamo-cortico-thalamic loops (Meeren et al., 2002), and thalamic activation has been reported in response to interictal discharges (Gotman et al., 2005).

Our findings provide a context for previous reports of altered oscillatory activity following VNS. For instance, previous authors have reported greater gamma power and synchronization following chronic stimulation (Marrosu et al., 2005). It is well-established that thalamo-cortical coherence promotes cortico-cortico synchronization (Sarnthein and Jeanmonod, 2007) and that thalamocortical cells spontaneously oscillate coherently with field potentials from related cortical regions within the gamma band (Nunez et al., 1992). The enhanced thalamo-cortical connectivity we report in patients who respond to VNS may facilitate band-limited coherence, providing a critical missing link between previously reported electrophysiological findings and patients outcomes.

We show that greater positive correlation between the thalamus and cortical regions that are implicated in thalamic outflow may identify patients who are most likely to benefit from stimulation. These findings suggest that the modulation of intrinsic pathways that are differentially expressed among individuals with epilepsy is associated with treatment response. At the behavioural level, it has been suggested in a large systematic review of the literature that patients with generalized seizure semiologies are more likely to become seizure-free with VNS (Englot et al., 2016). Various functional neuroimaging studies (Ibrahim et al., 2014a; Peng and Hsin, 2017), as well as electrophysiological investigations (Wolf and Beniczky, 2014) have conclusively implicated distinct thalamocortical circuitry in the generalization of seizure activities, including those related to the cingulate and insular cortices (Peng and Hsin, 2017). Our findings provide a putative connectomics-informed explanation of clinical observations in this patient population.

4.3. Large-scale connectomics to identify patients who may benefit from neuromodulation

The current study provides the first demonstration of the application of intrinsic connectivity to identify patients who may benefit from neuromodulation for epilepsy. The maintenance of the brain's intrinsic connectivity consumes the majority of its metabolic demands (Raichle and Mintun, 2006). Dysfunction of developing intrinsic connectivity networks has been previously linked to the clinical manifestations of epilepsy (Ibrahim et al., 2014a; Vaessen et al., 2012; Widjaja et al., 2013) as well as its neurocognitive comorbidities (Ibrahim et al., 2014a; Ibrahim et al., 2014b). Normative and compensatory patterns of functional connectivity have also been previously linked to post-operative neurocognitive function (McCormick et al., 2013). Very recently, a study of adults undergoing temporal lobectomy for intractable epilepsy demonstrated that centrality of the thalamus on pre-operative functional imaging was associated with post-operative seizure outcome (He et al., 2017), further buttressing the importance of large-scale connectivity within thalamocortical circuitry in the understanding and treatment of epilepsy.

Our results also complement findings in other diseases. The field of connectomics has expanded considerably in recent years as ongoing efforts attempt to cluster patients subgroups by shared signatures of brain dysfunction, rather than clinical symptoms or behavioural phenotypes (Drysdale et al., 2017; Clementz et al., 2016). For instance, in a cohort of 17 patients, Liston and colleagues report that the connectivity of the subgenual cingulate cortex connectivity identifies patients who improve clinically following subsequent transcranial magnetic stimulation for depression (Liston et al., 2014). Akin to the thalamus in epilepsy, the subgenual cingulate represents a target for deep brain stimulation in depression (Lozano et al., 2012). Additionally, intrinsic connectivity also predicted responses to medical treatment of depression in 17 patients examined by Chen and colleagues (Chen et al., 2007).

4.4. Limitations and future directions

A significant limitation of our study is the fact that some children required sedation while others did not. It is expected that sedation would affect thalamocortical connectivity and the findings of the resting-state study (Huang et al., 2014; Barttfeld et al., 2015; Gili et al., 2013). It is likely that the analysis was underpowered to identify differences in connectivity attributable to sedation effects, which are qualitatively visible in the statistical Z-maps. The possibility that sedation state may modify the relations among thalamocortical connectivity and outcome has not been excluded, although the two brain regions identified in the main results are consistently reproduced in the subgroup analyses and validated in an admittedly small external cohort.

Second, it is desirable to obtain longer resting-state studies, as reliability/similarity of these studies improves with increasing scan time from 5 min to 13 min (Birn et al., 2013). The shorter scan time in the current study may be a source of bias, although reliability was tested in a small external cohort from a second institution. While ICA denoising was performed to correct for nuisance signals, physiological parameters such as respiration and heart rate variability were not collected. These may also bias our data (van Houdt et al., 2010), although it is not expected that this bias would be related to seizure response. Given our hypothesis-driven approach, we also drew ROIs using anatomical T1 images. Future studies could explore thalamocortical connectivity using data-driven methodology, including group-ICA or graph theoretical analysis of pair-wise voxel correlations.

While it is foreseeable that differences in neurocognitive function, neurological deficits, epilepsy phenotypes and different combinations of antiepileptic drugs within our population may also confound the results of intrinsic connectivity, it is likely that the effect would be to introduce a Type II error and diminish significant associations. Indeed,

previous studies examining these relationships did not highlight an association between thalamocortical interactions involving the anterior cingulate or insular cortices in these features (Ibrahim et al., 2014a; Vaessen et al., 2012; Widjaja et al., 2013). Furthermore, we note that the distribution of our significant associations shows a wide range across the cohort, suggesting that our findings are robust and not driven by outliers in the data. Finally, our study encompasses only 21 children with 8 additional subjects as a prediction cohort. Although similar studies include comparable numbers (Widjaja et al., 2013), a future prospective cohort is required to validate these findings in order to examine the predictive ability of intrinsic connectivity to identify children who may benefit from vagal nerve stimulation.

5. Conclusions

Given the heterogeneity in outcomes following implantation of VNS in children with intractable epilepsy, there is a pressing need to define biomarkers that may identify patients who are most likely to benefit from intervention. Here, we report specific pre-operative patient phenotypes, measured using intrinsic connectivity that portend a better response to chronic vagus nerve stimulation. Enhanced connectivity within thalamocortical circuitry, involving the anterior cingulate and insular cortices – regions that are to known to receive projections from thalamic nuclei – was found to be associated with seizure response to VNS. Importantly, we demonstrate that functional connectomics may play an important translational role in directing patient-specific, personalized treatments following validation of these findings in prospective patient cohorts.

Conflicts of interest

None.

Appendix A. Supplementary data

Supplementary data to this article can be found online at https://doi.org/10.1016/j.nicl.2017.09.015.

References

Barttfeld, P., Bekinschtein, T.A., Salles, A., et al., 2015. Factoring the brain signatures of anesthesia concentration and level of arousal across individuals. Neuroimage Clin. 9, 385–391. https://doi.org/10.1016/j.nicl.2015.08.013.

Beckstead, R.M., Morse, J.R., Norgren, R., 1980. The nucleus of the solitary tract in the monkey: Projections to the thalamus and brain stem nuclei. J. Comp. Neurol. 190, 259–282.

Birn, R.M., Molloy, E.K., Patriat, R., et al., 2013. The effect of scan length on the reliability of resting-state fMRI connectivity estimates. NeuroImage 83, 550–558.

Chase, M.H., Sterman, B., Clemente, C.D., 1966. Cortical and to subcortical afferent vagal patterns stimulation of response. Exp. Neurol. 16, 36–49.

Chen, C., Ridler, K., Suckling, J., et al., 2007. Brain imaging correlates of depressive symptom severity and predictors of symptom improvement after antidepressant treatment. Biol. Psychiatry 62, 407–414.

Christianini, N., Shawe-Taylor, J., 2000. An Introduction to Support Vector Machines and Other Kernel-Based Learning Methods. Cambridge University Press, Cambridge, UK.

Clementz, B., Sweeney, J., Hamm, J., et al., 2016. Identification of distinct psychosis biotypes using brain-based biomarkers. Am. J. Psychiatr. 173 (4), 373–384.

Drysdale, A.T., Grosenick, L., Downar, J., et al., 2017. Resting-state connectivity biomarkers define neurophysiological subtypes of depression. Nat. Med. 23 (1), 28–38.

Englot, D.J., Rolston, J.D., Wright, C.W., Hassnain, K.H., Chang, E.F., 2016. Rates and predictors of seizure freedom with vagus nerve stimulation for intractable epilepsy. Neurosurgery 79 (3), 345–353.

Fisher, R., Salanova, V., Witt, T., et al., 2010. Electrical stimulation of the anterior nucleus of thalamus for treatment of refractory epilepsy. Epilepsia 51 (5), 899–908.

Gili, T., Saxena, N., Diukova, A., Murphy, K., Hall, J.E., Wise, R.G., 2013. The thalamus and brainstem act as key hubs in alterations of human brain network connectivity induced by mild propofol sedation. J. Neurosci. Off. J. Soc. Neurosci. 33 (9),

4024–4031.

Gotman, J., Grova, C., Bagshaw, A., Kobayashi, E., Aghakhani, Y., Dubeau, F., 2005. Generalized epileptic discharges show thalamocortical activation and suspension of the default state of the brain. Proc. Natl. Acad. Sci. U. S. A. 102 (42), 15236–15240.

He, X., Pustina, D., Sperling, M.R., Sharan, A.D., Tracy, J.I., 2017. Presurgical thalamic " hubness " predicts surgical outcome in temporal lobe epilepsy. Neurology 88 (24), 2285–2293.

Henry, T., Votaw, J., Pennell, P., et al., 1999. Acute blood flow changes and efficacy of vagus nerve stimulation in partial epilepsy. Neurology 52 (6), 1166–1173.

Henry, T.R., Bakay, R.A.E., Pennell, P.B., Epstein, C.M., Votaw, J.R., 2004. Brain blood-flow alterations induced by therapeutic vagus nerve stimulation in partial epilepsy: II. Prolonged effects at high and low levels of stimulation. Epilepsia 45 (9), 1064–1070.

van Houdt, P.J., Ossenblok, P.P.W., Boon, P.A.J.M., et al., 2010. Correction for pulse height variability reduces physiological noise in functional MRI when studying spontaneous brain activity. Hum. Brain Mapp. 31, 311–325.

Huang, J., Wang, Z., Zhang, J., et al., 2014. Altered temporal variance and neural synchronization of spontaneous brain activity in anesthesia. Hum. Brain Mapp. 35, 5368–5378.

Ibrahim, G., Morgan, B., Lee, W., et al., 2014a. Impaired development of intrinsic connectivity networks in children with medically intractable localization-related epilepsy. Hum. Brain Mapp. 35, 5686–5700.

Ibrahim, G., Cassel, D., Morgan, B., et al., 2014b. Resilience of developing brain networks to interictal epileptiform discharges is associated with cognitive outcome. Brain 137, 2690–2702.

Ibrahim, G.M., Morgan, B.R., Lou, M., et al., 2015. Thalamocortical connectivity is enhanced following functional hemispherotomy for intractable lateralized epilepsy. Epilepsy Behav. 51, 281–285.

Jenkinson, M., Bannister, P., Brady, M., Smith, S., 2002. Improved optimization for the robust and accurate linear registration and motion correction of brain images. NeuroImage 17 (2), 825–841.

Kelly, R.E., Alexopoulos, G.S., Wang, Z., et al., 2010. Visual inspection of independent components: Defining a procedure for artifact removal from fMRI data. J. Neurosci. Methods 189 (2), 233–245.

Klinkenberg, S., Van den Bosch, C.N.C.J., Majoie, H.J.M., et al., 2012. Behavioural and cognitive effects during vagus nerve stimulation in children with intractable epilepsy: a randomized controlled trial. Eur. J. Paediatr. Neurol. 17 (1), 82–90.

Ko, D., Heck, C., Grafton, S., et al., 1996. Vagus nerve stimulation activates central nervous system structures in epileptic patients during PET H215O blood flow imaging. Neurosurgery 39 (2), 426–431.

Liston, C., Chen, A., Zebley, B., et al., 2014. Default mode network mechanisms of transcranial magnetic stimulation in depression. Biol. Psychiatry 76 (7), 517–526. http://dx.doi.org/10.1016/j.biopsych.2014.01.023.Default.

Liu, W., Mosier, K., Kalnin, A., Marks, D., 2003. BOLD fMRI activation induced by vagus nerve stimulation in seizure patients. J. Neurol. Neurosurg. Psychiatry 74, 811–814.

Lozano, A., PG, Hamani, C., et al., 2012. A multicenter pilot study of subcallosal cingulate area deep brain stimulation for treatment-resistant depression. J. Neurosurg. 116, 315–322.

Marrosu, F., Santoni, F., Puligheddu, M., et al., 2005. Increase in 20–50 Hz (gamma frequencies) power spectrum and synchronization after chronic vagal nerve stimulation. Clin. Neurophysiol. 116 (9), 2026–2036.

McCormick, C., Quraan, M., Cohn, M., Valiante, T.A., McAndrews, M.P., 2013. Default mode network connectivity indicates episodic memory capacity in mesial temporal lobe epilepsy. Epilepsia 54 (5), 809–818.

Meeren, H.K., Pijn, J.P., van Luijtelaar, E.L., Coenen, A.M., da Silva, F.H.L., 2002. Cortical foc spontaneous absence seizures in rats. J. Neurosci. 22 (4), 1480–1495.

Narayanan, J.T., Watts, R., Haddad, N., Labar, D.R., Li, P.M., Filippi, C.G., 2002. Cerebral activation during vagus nerve stimulation: a functional MR study. Epilepsia 43 (12), 1509–1514.

Naritoku, D., Morales, A., Pencek, T., Winkler, D., 1992. Chronic vagus nerve stimulation increases the latency of the thaiamocortical somatosensory evoked potential. Pacing Clin. Electrophysiol. 15 (10 Pt 2), 1572–1579.

Naritoku, D.K., Terry, W.J., Helfert, R.H., 1995. Regional induction of fos immunoreactivity in the brain by anticonvulsant stimulation of the vagus nerve. Epilepsy Res. 22, 53–62.

Nunez, A., Amzica, F., Steriade, M., 1992. Intrinsic and synaptically generated delta (1–4 Hz) rhythms in dorsal lateral geniculate neurons and their modulation by light-induced fast (30–70 Hz) events. Neuroscience 51 (2), 269–284.

Panebianco, M., Rigby, A., Weston, J., Ag, M., 2015. Vagus nerve stimulation for partial seizures. Cochrane Database Syst. Rev. 2015 (4), 1–47.

Peng, S., Hsin, Y., 2017. Clinical altered structural and functional thalamocortical networks in secondarily generalized extratemporal lobe seizures. Neuroimage Clin. 13, 55–61.

Raichle, M.E., Mintun, M.A., 2006. Brain work and brain imaging. Annu. Rev. Neurosci. 29, 449–476.

Rutecki, P., 1990. Anatomical, physiological, and theoretical basis for the antiepileptic effect of vagus nerve stimulation. Epilepsia 31 (Suppl. 2), S1–6.

Saleh, T., Cechetto, F., 1993. Peptides in the parabrachial nucleus modulate visceral input to the thalamus. Am. J. Phys. 264 (4 Pt 2), R668–75.

Sarnthein, J., Jeanmonod, D., 2007. High thalamocortical theta coherence in patients with Parkinson's disease. J. Neurosci. 27 (1), 124–131.

Vaessen, M.J., Braakman, H.M., Heerink, J.S., et al., 2012. Abnormal modular organization of functional networks in cognitively impaired children with frontal lobe epilepsy. Cereb. Cortex 23 (8), 1997–2006.

Widjaja, E., Zamyadi, M., Raybaud, C., Snead, O.C., Smith, M.L., 2013. Impaired Default Mode Network on Resting-State fMRI in Children with Medically Refractory Epilepsy. AJNR Am. J. Neuroradiol. 34 (3), 552–557.

Wolf, P., Beniczky, S., 2014. Understanding ictogenesis in generalized epilepsies. Expert. Rev. Neurother. 14 (7), 787–798.

Woolrich, M.W., Ripley, B.D., Brady, M., Smith, S.M., 2001. Temporal autocorrelation in univariate linear modeling of FMRI data. NeuroImage 14 (6), 1370–1386.

Worsley, K.J., 2001. Statistical analysis of activated images. In: Jezzard, P., Matthews, P.M., Smith, S.M. (Eds.), Functional MRI: An Introduction to Methods. OUP (Chapter 14).

Zhang, D., Raichle, M.E., 2010. Disease and the brain's dark energy. Nat. Rev. Neurol. 6 (1), 15–28.